

# Steering Epitaxial Alignment of Au, Pd, and AuPd Nanowire Arrays by Atom Flux Change

Youngdong Yoo,<sup>†</sup> Kwanyong Seo,<sup>†</sup> Sol Han,<sup>†</sup> Kumar S. K. Varadwaj,<sup>†</sup> Hyun You Kim,<sup>†</sup> Ji Hoon Ryu,<sup>‡</sup> Hyuck Mo Lee,<sup>‡</sup> Jae Pyoung Ahn,<sup>§</sup> Hyotcherl Ihee,<sup>†</sup> and Bongsoo Kim<sup>\*,†</sup>

<sup>†</sup>Department of Chemistry, <sup>‡</sup>Department of Materials Science and Engineering, KAIST, Daejeon 305-701, Korea, and <sup>§</sup>Nano-Material Research Center, KIST, Seoul 136-791, Korea

**ABSTRACT** We have synthesized epitaxial Au, Pd, and AuPd nanowire arrays in vertical or horizontal alignment on a c-cut sapphire substrate. We show that the vertical and horizontal nanowire arrays grow from half-octahedral seeds by the correlations of the geometry and orientation of seed crystals with those of as-grown nanowires. The alignment of nanowires can be steered by changing the atom flux. At low atom deposition flux vertical nanowires grow, while at high atom flux horizontal nanowires grow. Similar vertical/horizontal epitaxial growth is also demonstrated on SrTiO<sub>3</sub> substrates. This orientation-steering mechanism is visualized by molecular dynamics simulations.

**KEYWORDS** Gold, palladium, nanowire, epitaxial growth, seed crystal

Precisely controlled growth of nanowires (NWs) on a substrate along a chosen crystallographic direction has been greatly sought in nanotechnology.<sup>1–11</sup> This would allow for integration of one-dimensional building blocks into a designed system and mass production of nanodevices from bottom-up approach. So far epitaxial alignment of NWs has been determined by the crystal orientation of the substrate.<sup>12–16</sup> Selection of the alignment (whether vertical or horizontal) of NWs on the same substrate by only adjusting the reaction conditions would be more desirable and help provide fabrication of more versatile three-dimensional nanodevices.

Noble metal NWs have attracted much attention because of their unique optical, catalytic, sensing, and electronic properties.<sup>17</sup> Although a large number of reports on the synthesis of noble metal NWs are available,<sup>18–21</sup> epitaxial growth of noble metal NWs has not been reported yet. Epitaxially aligned noble metal NW arrays on a substrate can be utilized as advanced platforms for plasmonics, optoelectronics, sensing, selective catalytic reactions, and nanoelectronics.<sup>22–26</sup>

Here we show for the first time that we can epitaxially grow noble metal (Au, Pd, and AuPd) NW arrays in a selected alignment without using any catalysts or capping reagents. Furthermore, we show that the alignment of NWs (vertical or horizontal) can be steered by changing the atom flux on the same substrate. How these metals with an isotropic crystal structure (face-centered cubic) can grow into aligned NW arrays without using any catalysts or templates? How their alignment can be steered by atom flux change? As an answer to these

intriguing questions, we present a detailed mechanism for the vertical and horizontal epitaxial growth of Au NWs.

The Au NWs are synthesized by a simple vapor transport method<sup>27</sup> using a Au slug as a metal source. Vertical Au NWs are grown on a c-cut sapphire substrate at a source temperature of 1100 °C. Figure 1a shows a scanning electron microscope (SEM) image (tilted 45°) of vertical Au NWs. The NWs have diameters of 90–190 nm and lengths of 10–20 μm. The transmission electron microscope (TEM) images and selected area electron diffraction (SAED) patterns confirm that these Au NWs are single crystalline without twins or defects and grow along the [110] direction (Supporting Information, Figure S1 and S2). Magnified images in Figure 1b show that the Au NWs are well-faceted and have grown in three orientations at angles 120° (or 60°) to one another with their top edges having a [110] direction parallel to the substrate. These three orientations of the Au NWs are consistent with the 3-fold symmetry of c-cut sapphire. Each NW is an elongated half-octahedron, made up of four {111} side facets, two {111} top facets consisting of equilateral triangular planes, and a (110) bottom surface with the epitaxial relationship between vertical NWs and sapphire of (110) Au// (0001) sapphire.

The key experimental conditions affecting the growth process are the deposition flux (number of Au atoms deposited per unit time and unit area), substrate temperature, and local flow conditions.<sup>28</sup> The values of these parameters strongly depend on the location on the substrate, leading to distributions of various nanostructures on the substrate. Among the nanostructures grown on the substrate, we have identified half-octahedral Au nanocrystals as the seeds of vertical NWs. Figure 1c shows a top-view image of the half-octahedral Au nanocrystals observed at different locations on one same substrate. These particles are also aligned in three orientations at 120° to one another. Figure 1b,d shows

\* To whom correspondence should be addressed. E-mail: bongsoo@kaist.ac.kr.  
Tel: +82-42-350-2836. Fax: +82-42-350-2810.

Received for review: 09/10/2009

Published on Web: 01/05/2010

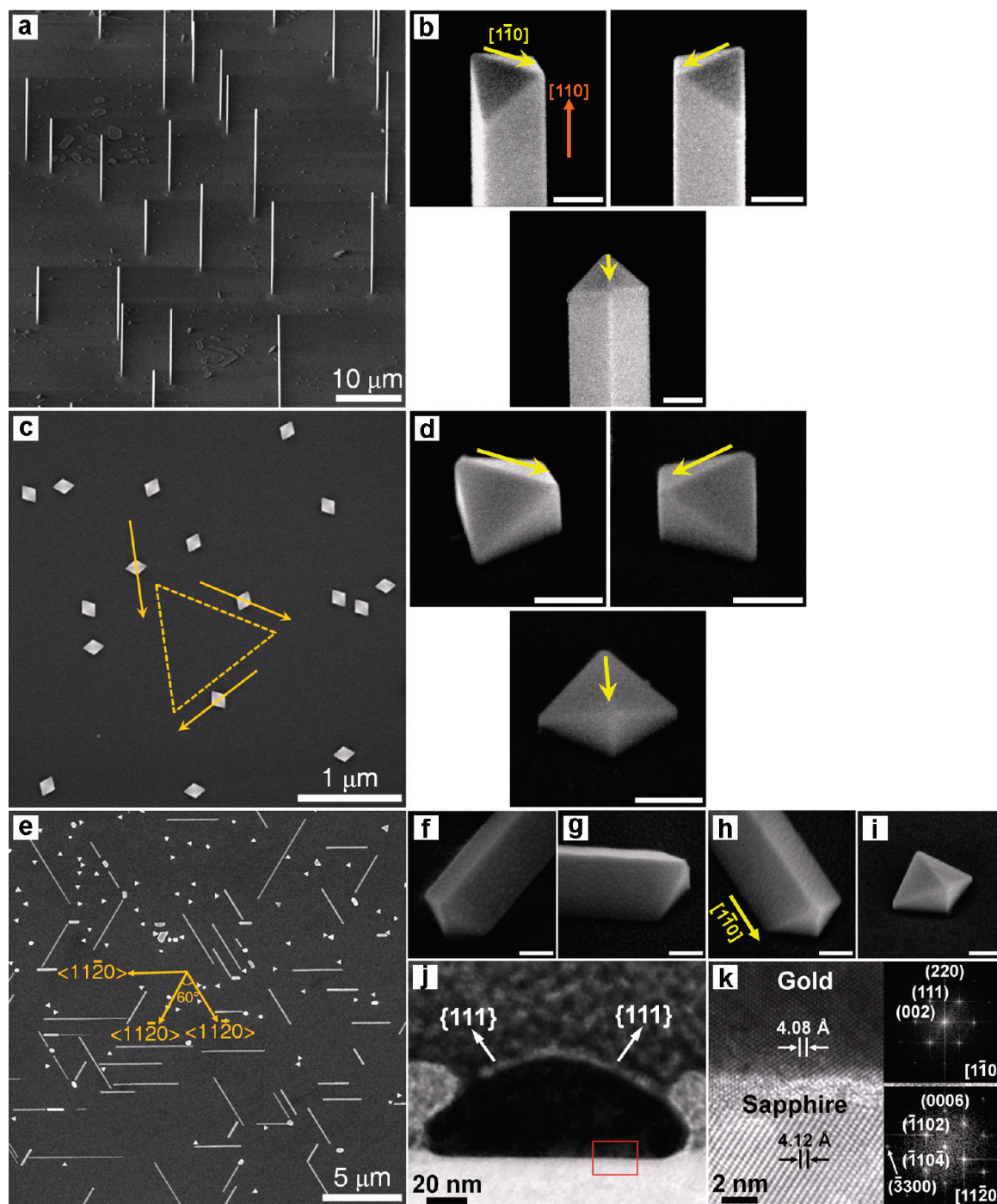


**FIGURE 1.** Vertically and horizontally grown Au NWs and their half-octahedral seeds on c-cut sapphire substrates. (a) 45° tilted SEM image of vertical NWs. (b) Magnified SEM images of (a). The NWs have three orientations at 120° to one another. Yellow arrows indicate the three top edges with a  $[1\bar{1}0]$  direction parallel to the substrate. (c) Top-view SEM image of Au seeds aligned in three orientations at 120° to one another (indicated by arrows and a triangle). (d) Magnified and 45° tilted SEM images of half-octahedral Au seeds in three orientations. Yellow arrows indicate the three top edges with a  $[110]$  direction. (e) Top-view SEM image of horizontal NWs grown along three  $\langle 11\bar{2}0 \rangle$  directions of sapphire. (f–h) Magnified and 45° tilted SEM images of horizontal NWs. (i) Magnified and 45° tilted SEM image of a half-octahedral seed in the same orientation as (h). (j) Cross-sectional TEM image of the horizontal NW grown on c-cut sapphire. (k) HRTEM image and FFT patterns of the red square in (j). The lattice spacing of the Au (100) planes is 4.08 Å, and that of sapphire (1010) planes is 4.12 Å (mismatch 0.98%). Scale bars in (b,d,f–i) are 100 nm.

that the orientations of these half-octahedral nanocrystals are the same as those of the vertical NWs. The strong correlation of the geometry and orientations of the half-

octahedral nanocrystals with those of the vertical NWs indicates that the vertical Au NWs grow from the half-octahedral Au nanocrystals.

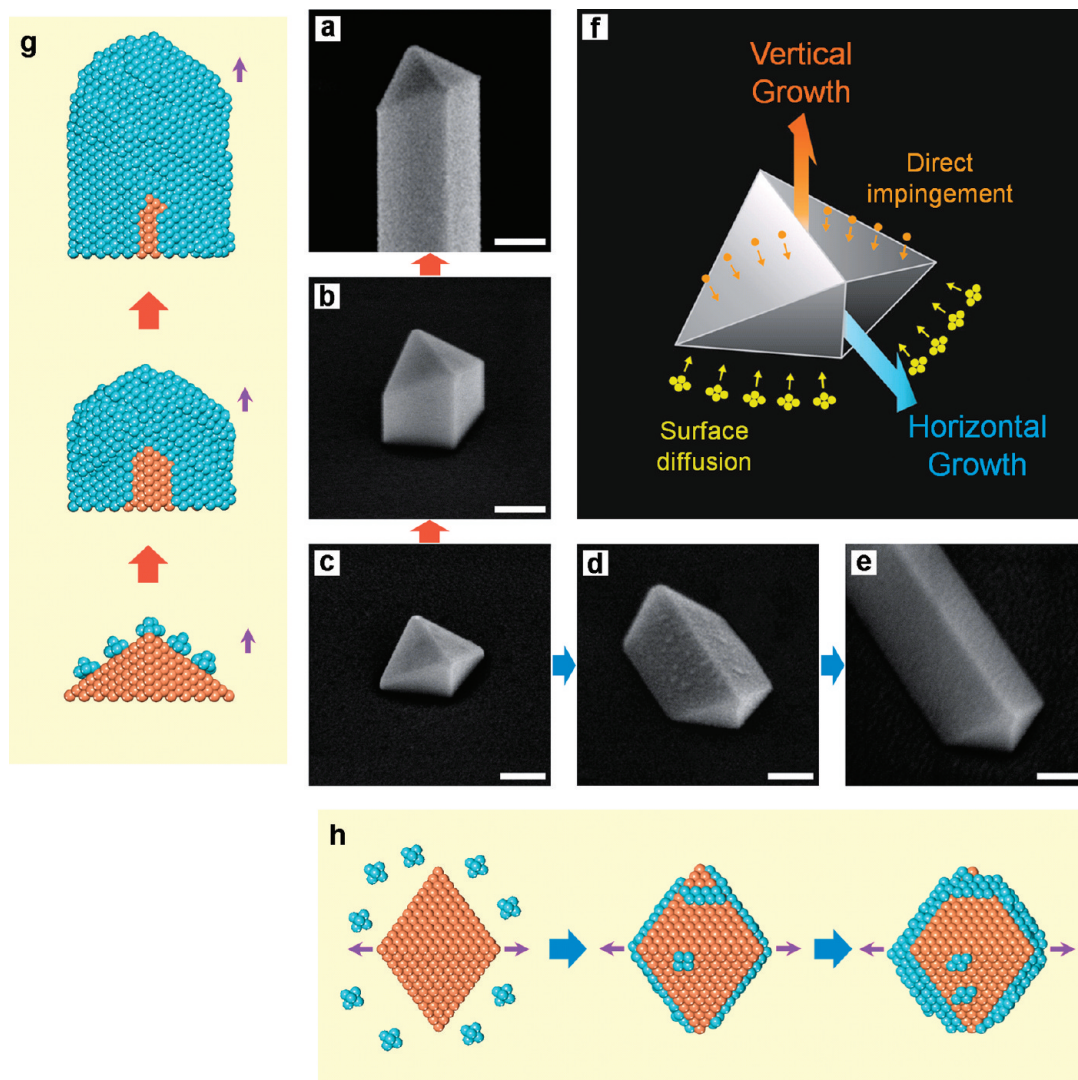


**FIGURE 2.** The growth process of Au NWs from half-octahedral seeds on c-cut sapphire substrates. Panels a–e show 45° tilted SEM images from the same perspective. (a,b) Vertically grown Au NWs. (c) A half-octahedral Au seed. (d,e) Horizontally grown Au NWs. Vertical NWs (a,b) are obtained at a source temperature of 1100 °C whereas horizontal NWs (d,e) are obtained at 1300 °C. (f) Schematic for Au NW growth model. (g) MD simulated images of the vertical growth from a half-octahedral seed by direct impingement as seen from the side (see Supporting Information, Movie S1). (h) MD simulated images of the horizontal growth from a half-octahedral seed by surface diffusion as seen from the top (see Supporting Information, Movie S2). Scale bars in (a–e) are 100 nm.

When we raise the source temperature to 1300 °C, we observe horizontal rather than vertical NWs (Figure 1e). These NWs grow along the three equivalent  $\langle 11\bar{2}0 \rangle$  directions of sapphire rotated by 120° on the basal c plane. Figure 1f–h shows the geometry of the horizontal NWs. Half-octahedral nanocrystals aligned in the same three orientations as the horizontal NWs are also found on the same substrate (compare Figure 1h,i), suggesting that the horizontal NWs grow from half-octahedral nanocrystals. The cross-sectional TEM image shows that the horizontal NWs have triangular cross sections (Figure 1j). The high-resolution TEM (HRTEM) image and its fast Fourier transform (FFT) patterns (Figure 1k) reveal that the horizontal NWs have all  $\{111\}$  facets except a (110) bottom surface. Thus, the epitaxial relationship between the horizontal NWs and sapphire is also (110) Au// (0001) sapphire.

If the seed is half-octahedral, only when the NWs grow along the  $\langle 110 \rangle$  directions, they would be enclosed by the most stable  $\{111\}$  top and side facets.<sup>29</sup> Growth to other direction would lead to formation of less stable facets. NW growth from a half-octahedral seed is thereby confined to either a vertical or horizontal direction. The three orientations of the vertical and horizontal NWs arise from the initial nucleation of half-octahedral seeds in three orientations. An identical epitaxial relationship of the vertical and horizontal NWs with c-cut sapphire confirms that both NWs grow from the same half-octahedral seed.

Figure 2 illustrates that half-octahedral seeds can grow into NWs along two different paths:  $c \rightarrow b \rightarrow a$  and  $c \rightarrow d \rightarrow e$  for source temperatures of 1100 °C and 1300 °C, respectively. The Au deposition flux at 1300 °C is about 50 times higher

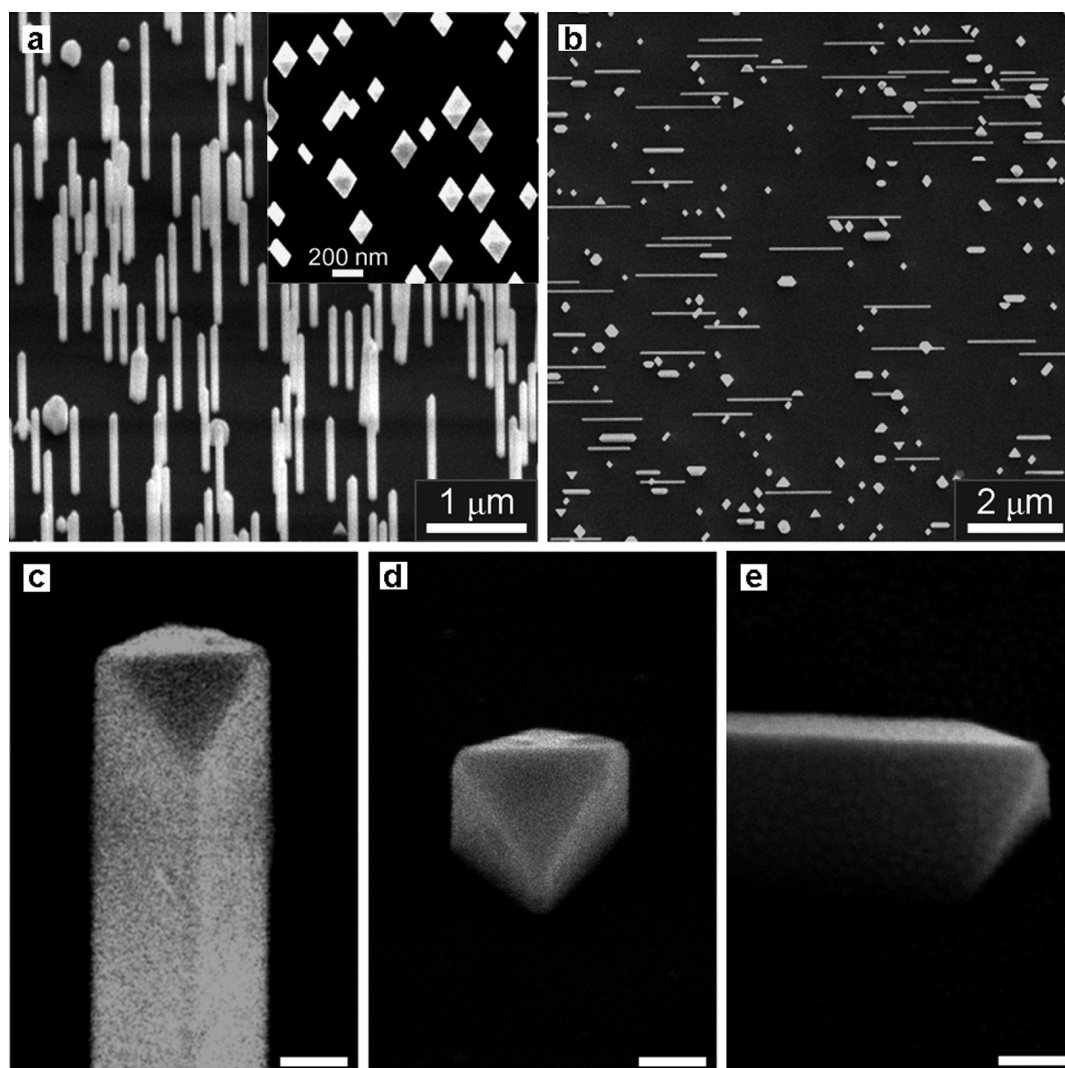


FIGURE 3. Vertically and horizontally grown Au NWs on Nb-doped SrTiO<sub>3</sub> (110) substrates. (a) 45° tilted SEM image of vertical Au NWs grown at a source temperature of 1,100 °C. The inset shows a top-view SEM image of vertical NWs. (b) Top-view SEM image of horizontal Au NWs grown at a source temperature of 1,250 °C. NWs grow horizontally along one direction because of the 2-fold symmetry of the Nb-doped SrTiO<sub>3</sub> (110) substrate. 45° tilted magnified SEM images of (c) the vertical NW, (d) the half-octahedral seed, and (e) the horizontal NW. The temperatures of the substrates were both maintained at 1,000 °C and all other reaction conditions (e.g., pressure, and Ar flow rate) were the same in the two experiments. The distance from the center of the heating zone to the center of the substrate was 5.3 cm for the 1100 °C experiment (low flux) and 7.9 cm for the 1,250 °C experiment (high flux). Scale bars in (c–e) are 50 nm.

than that at 1100 °C, as estimated from the Au vapor pressure.<sup>30</sup> All other experimental parameters are kept identical. We thus deduce that the magnitude of the deposition flux determines whether the growth from the half-octahedral seed will be vertical or horizontal.

Among the possible NW growth mechanisms, we can exclude screw dislocation-driven growth because no dislocation is observed in the Au NWs.<sup>51,52</sup> We also exclude vapor–liquid–solid and vapor–solid–solid growth because no catalyst is used in these experiments.<sup>53–57</sup> We propose the following explanation for the observed orientation-steering growth. Anisotropic growth can be induced by an anisotropic environment that provides anisotropic flows of material to the seed crystal.<sup>38</sup> In our experiments, the magnitude of the deposition flux determines the dominant

material flux direction toward the seed, which in turn steers the NW growth direction. Gold atoms colliding with the substrate will diffuse and nucleate to form small seed crystals aligned along the orientation of the substrate (Figure 1c,d). Au atoms are supplied to the seed by direct impingement from the vapor or by surface diffusion.

In the low deposition flux regime, Au atoms colliding with the substrate diffuse either alone or as a small cluster of a few Au atoms, desorbing easily. Thus, Au atoms reaching seed crystals via diffusion will be greatly outnumbered by those colliding with the seed by direct impingement. The situation is reversed in the high deposition flux regime. As the deposition flux increases, the aggregation rate of Au atoms increases nonlinearly to form large clusters that do not desorb easily and diffuse at a rate comparable to that

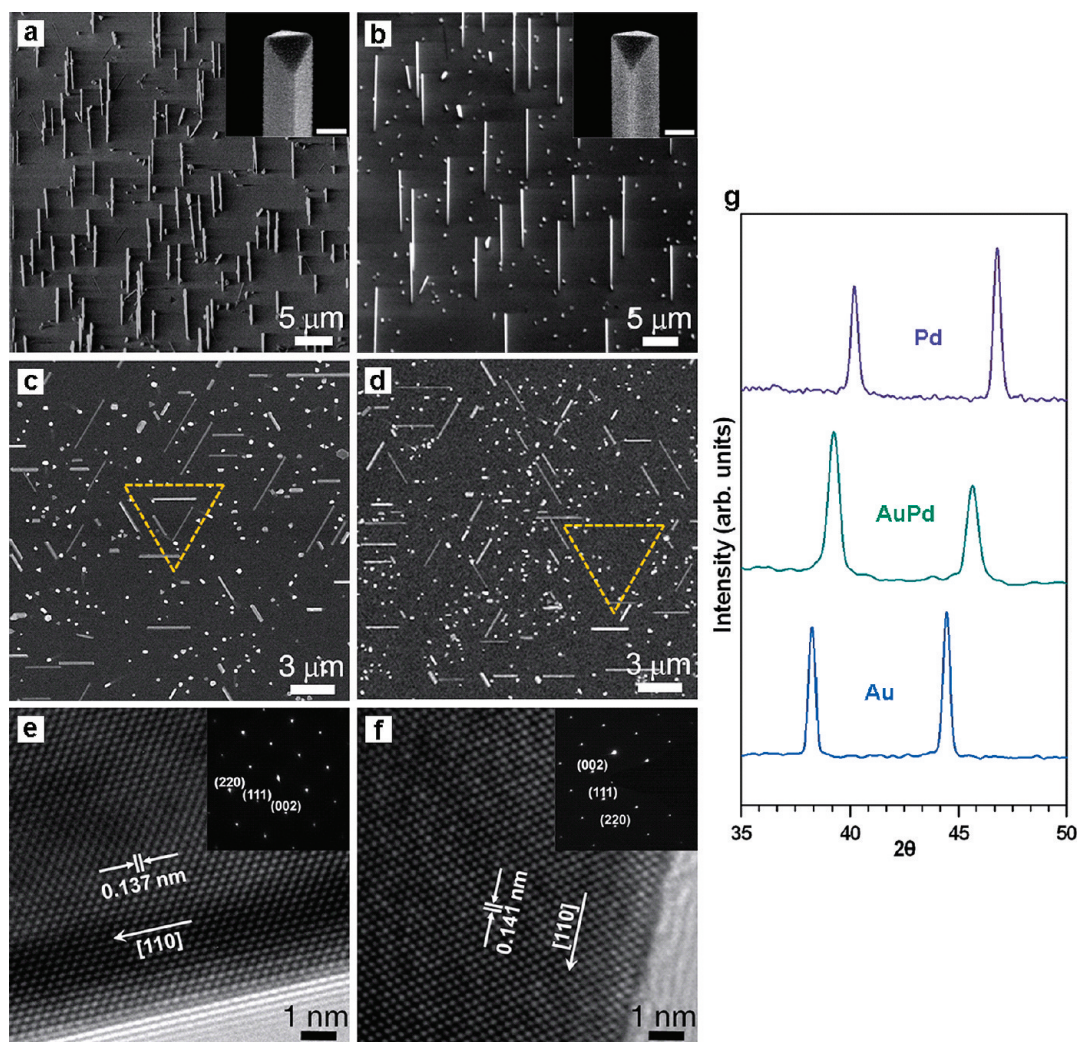


FIGURE 4. Vertically and horizontally grown Pd and AuPd NWs on c-cut sapphire substrates. 45° tilted SEM images of vertical NWs (a) for Pd and (b) for AuPd. The insets are magnified images showing the tip shape. Top-view SEM images of horizontal NWs aligned in three orientations at 120° to one another (c) for Pd and (d) for AuPd. HRTEM images and SAED patterns of the NWs (e) for Pd and (f) for AuPd. (g) XRD patterns of Pd, AuPd, and Au NWs grown on c-cut sapphire substrates. The peaks corresponding to the (111) and (200) planes of the fcc Pd, AuPd, Au crystal structure are shifted to a higher d-value (lower  $2\theta$  value) as we move from Pd to AuPd and Au. Scale bars of the insets in (a,b) are 100 nm.

for adatoms.<sup>39</sup> Since the area of the substrate from which the diffusing atoms are collected by the seed is much larger than that of the top face of a seed to which atoms directly impinge, the atom supply to the seed will be dominated by surface diffusion rather than by direct impingement. The NW growth rate induced by surface diffusion would increase more rapidly with the increase of deposition flux than that induced by direct impingement.

While Au atoms directly impinging to the half-octahedral seed contribute mostly to the vertical growth, the diffusing atoms (or clusters) arriving at a vertical side face of the half-octahedral seed (forming a reentrant edge) contribute mostly to horizontal growth.<sup>40</sup> Consequently, vertical growth dominates when Au is supplied largely by direct impingement (low flux regime), and horizontal growth dominates when surface diffusion is the major supply of Au atoms (high flux

regime). A schematic illustrating this explanation is shown in Figure 2f.

Our interpretation of the observed growth behavior is consistent with the results from molecular dynamics (MD) simulations presented in Figure 2g,h. The MD simulations were carried out at 800 K using a canonical ensemble. A half-octahedral Au seed composed of 614 atoms was fixed onto a double layer graphite support. Relevant potential parameters of Au were described by a quantum Sutton–Chen potential.<sup>41</sup> The interaction between Au and C atoms was parametrized with a 12-6 Lennard-Jones potential.<sup>42</sup> Initially, 20 Au clusters composed of 5 atoms each were placed 0.5 nm above the top of the seed crystal or distributed on the surface of a supporting layer freely to simulate direct impingement or adatom diffusion, respectively. Additional 100 Au atoms (20 Au clusters composed

of 5 atoms each) were continuously added to the system in every ns of simulation time.

We took graphite as a supporting layer to reduce computation time. Graphite is a typical supporting material for metal clusters.<sup>43</sup> Moreover, Au–C interaction is not too strong to prevent the surface diffusion of Au adatoms at the reaction temperature.<sup>44</sup> We constructed two contrastive simulation models to illustrate the influence of direct impingement and adatom diffusion on the directional growth of Au seed crystals. It is remarkable that directly impinged Au clusters were spread out to form a (111) layer. After redistribution, each atom created a surface layer on top of the Au seed. The range of dynamic movement of impinging atoms was restricted to the surface layer of the seed. Continuous addition of Au atoms on the top layer resulted in vertical NW growth. For the simulation of horizontal surface diffusion, freely distributed Au clusters on the surface of the supporting layer approached and coalesced with the seed leading to horizontal NW growth as the simulation proceeded.

Vertical NW growth is illustrated in Figure 2g and Supporting Information, Movie S1. Horizontal NW growth is illustrated in Figure 2h and Supporting Information, Movie S2. The images in Figure 2g,h are snapshots obtained by MD simulations during direct impingement and surface diffusion, respectively, of the Au atoms. Although the Au atoms in practice are always supplied from both directions, if the supply from one direction is much larger than the other, the seed grows toward the dominant Au flux.

This seed-initiated orientation-steering growth of Au NWs is successfully employed on other substrates. Figure 3a shows a 45° tilted SEM image of Au NW arrays on an Nb-doped SrTiO<sub>3</sub> (110) substrate, synthesized at a source temperature of 1100 °C. Interestingly, the orientations of the NWs are all identical (inset in Figure 3a). This is due to the 2-fold symmetry of the Nb-doped SrTiO<sub>3</sub> (110) substrate. The equilibrium shape of a metal nanoparticle crystallized on a substrate is determined by the surface energy of the crystal facets and the interface energy between the crystal and the substrate.<sup>45</sup> The c-cut sapphire and the SrTiO<sub>3</sub> (110) have favorable lattice match with the half-octahedral Au seed (Supporting Information, Figure S4), leading to formation of well-oriented half-octahedral seed consistent with the crystal symmetry of the substrate (3-fold in c-cut sapphire or 2-fold in SrTiO<sub>3</sub> substrates). The growth direction of Au NWs (either vertical or horizontal) was also steered by redirecting the dominant material flux toward the seed. When we raise the source temperature to 1250 °C, we observe horizontal rather than vertical NWs (Figure 3b). All other reaction conditions except source temperature were the same in the two experiments. Half-octahedral seeds aligned in the same orientation as the vertical and horizontal NWs are also found on the same substrate (compare Figure 3c, 3d and 3e).

We have achieved similar seed-crystal-initiated orientation-steering growth of Pd and AuPd NWs on c-cut sap-

phire substrates. Synthesis of these twin-free, single-crystalline, and well-faceted Pd and AuPd NWs on the substrate has not been previously reported. Vertical Pd and AuPd alloy NWs are grown at a source temperature of 1100 °C (Figure 4a,b). When the source temperature is raised to 1300 °C, horizontal NWs of Pd and AuPd are obtained (Figure 4c,d). The HRTEM images and SAED patterns of the Pd and AuPd NWs (Figure 4e,f) are fully indexed to fcc Pd and AuPd structures with lattice constants 3.890 and 3.983 Å, respectively,<sup>46</sup> and show that the NWs have single crystalline nature and a [110] growth direction. The lattice spacing of the planes parallel to the growth direction is calculated to be 0.137 and 0.141 nm, agreeing well with the spacing of the (110) planes of fcc Pd and AuPd structures, respectively. These observations indicate that the growth mechanisms of the Pd and AuPd NWs are very similar to that of the Au NWs.

We have demonstrated the orientation-steering growth of Au, Pd, and AuPd NWs on a substrate without catalysts and have proposed a new mechanism explaining how the NWs grow from seed crystals. The growth direction of NWs can be steered by redirecting the dominant atom supply flux toward seed crystals formed epitaxially on a substrate. By employing this seed-crystal-initiated growth, it would be possible to fabricate more versatile three-dimensional NW devices as well as to induce aligned epitaxial growth of NWs from new materials.

**Acknowledgment.** We thank NRF for support through the NRL (20090083138) and Nano Research and Development (R&D) program (20090083221) and the Center for Nanostructured Materials Technology (2009K000468) under the 21c Frontier R&D program of the MEST, Korea. We thank J. W. Lee for helpful discussions.

**Supporting Information Available.** Detailed descriptions of materials and methods, supplementary figures, supplementary discussions, and supplementary movies. This material is available free of charge via the Internet at <http://pubs.acs.org>.

## REFERENCES AND NOTES

- (1) Kuykendall, T.; Pauzauskie, P. J.; Zhang, Y.; Goldberger, J.; Sirbuly, D.; Denlinger, J.; Yang, P. *Nat. Mater.* **2004**, *3*, 524.
- (2) Bakkers, E. P. A. M.; Dam, J. A. V.; Franceschi, S. D.; Kouwenhoven, L. P.; Kaiser, M.; Verheijen, M.; Wondergem, H.; Sluis, P. V. D. *Nat. Mater.* **2004**, *3*, 769.
- (3) Ng, H. T.; Li, J.; Smith, M. K.; Nguyen, P.; Cassell, A.; Han, J.; Meyyappan, M. *Science* **2003**, *300*, 1249.
- (4) Aagesen, M.; Johnson, E.; Sørensen, C. B.; Mariager, S. O.; Feidenhans'l, R.; Spiecker, E.; Nygård, J.; Lindelof, P. E. *Nat. Nanotechnol.* **2007**, *2*, 761.
- (5) Gao, L.; Woo, R. L.; Liang, B.; Pozuelo, M.; Prikhodko, S.; Jackson, M.; Goel, N.; Hudait, M. K.; Huffaker, D. L.; Goorsky, M. S.; Kodambaka, S.; Hicks, R. F. *Nano Lett.* **2009**, *9*, 2223.
- (6) Woodruff, J. H.; Ratchford, J. B.; Goldthorpe, I. A.; McIntyre, P. C.; Chidsey, C. E. D. *Nano Lett.* **2007**, *7*, 1637.
- (7) Jensen, L. E.; Björk, M. T.; Jeppesen, S.; Persson, A. I.; Ohlsson, B. J.; Samuelson, L. *Nano Lett.* **2004**, *4*, 1961.
- (8) Woo, R. L.; Gao, L.; Goel, N.; Hudait, M. K.; Wang, K. L.; Kodambaka, S.; Hicks, R. F. *Nano Lett.* **2009**, *9*, 2207.

- (9) Chung, H.-S.; Jung, Y.; Kim, S. C.; Kim, D. H.; Oh, K. H.; Agarwal, R. *Nano Lett.* **2009**, *9*, 2395.
- (10) Huang, Z.; Shimizu, T.; Senz, S.; Zhang, Z.; Zhang, X.; Lee, W.; Geyer, N.; Gösele, U. *Nano Lett.* **2009**, *9*, 2519.
- (11) Wei, W.; Bao, X.-Y.; Soci, C.; Ding, Y.; Wang, Z.-L.; Wang, D. *Nano Lett.* **2009**, *9*, 2926.
- (12) Sohn, J. I.; Joo, H. J.; Porter, A. E.; Choi, C.-J.; Kim, K.; Kang, D. J.; Welland, M. E. *Nano Lett.* **2007**, *7*, 1570.
- (13) Hsu, H.-C.; Wu, W.-W.; Hsu, H.-F.; Chen, L.-J. *Nano Lett.* **2007**, *7*, 885.
- (14) Mandl, B.; Stangl, J.; Mårtensson, T.; Mikkelsen, A.; Eriksson, J.; Karlsson, L. S.; Bauer, G.; Samuelson, L.; Seifert, W. *Nano Lett.* **2006**, *6*, 1817.
- (15) Adhikari, H.; Marshall, A. F.; Chidsey, C. E. D.; McIntyre, P. C. *Nano Lett.* **2006**, *6*, 318.
- (16) Ge, S.; Jiang, K.; Lu, X.; Chen, Y.; Wang, R.; Fan, S. *Adv. Mater.* **2005**, *17*, 56.
- (17) Murphy, C. J.; Sau, T. K.; Gole, A. M.; Orendorff, C. J.; Gao, J.; Gou, L.; Hunyadi, S. E.; Li, T. *J. Phys. Chem. B* **2005**, *109*, 13857.
- (18) Wang, C.; Hu, Y.; Lieber, C. M.; Sun, S. *J. Am. Chem. Soc.* **2008**, *130*, 8902.
- (19) Huo, Z.; Tsung, C.-k.; Huang, W.; Zhang, X.; Yang, P. *Nano Lett.* **2008**, *8*, 2041.
- (20) Li, Z.; Tao, J.; Lu, X.; Zhu, Y.; Xia, Y. *Nano Lett.* **2008**, *8*, 3052.
- (21) Kim, F.; Sohn, K.; Wu, J.; Huang, J. *J. Am. Chem. Soc.* **2008**, *130*, 14442.
- (22) Nagpal, P.; Lindquist, N. C.; Oh, S.-H.; Norris, D. J. *Science* **2009**, *325*, 594.
- (23) Huang, M. H.; Mao, S.; Feick, H.; Yan, H.; Wu, Y.; Kind, H.; Weber, E.; Russo, R.; Yang, P. *Science* **2001**, *292*, 1897.
- (24) Favier, F.; Walter, E. C.; Zach, M. P.; Benter, T.; Penner, R. M. *Science* **2001**, *293*, 2227.
- (25) Komanicky, V.; Iddir, H.; Chang, K.-C.; Menzel, A.; Karapetrov, G.; Hennessy, D.; Zapol, P.; You, H. *J. Am. Chem. Soc.* **2009**, *131*, 5732.
- (26) Huang, Y.; Duan, X.; Wei, Q.; Lieber, C. M. *Science* **2001**, *291*, 630.
- (27) Dai, Z. R.; Pan, Z. W.; Wang, Z. L. *Adv. Funct. Mater.* **2003**, *13*, 9.
- (28) Röder, H.; Hahn, E.; Brune, H.; Bucher, J. P.; Kern, K. *Nature* **1993**, *366*, 141.
- (29) Vitos, L.; Ruban, A. V.; Skriver, H. L.; Kollar, J. *Surf. Sci.* **1998**, *411*, 186.
- (30) Ward, J. W. *J. Chem. Phys.* **1967**, *47*, 4030.
- (31) Bierman, M. J.; Lau, Y. K. A.; Kvit, A. V.; Schmitt, A. L.; Jin, S. *Science* **2008**, *320*, 1060.
- (32) Zhu, J.; Peng, H.; Marshall, A. F.; Barnett, D. M.; Nix, W. D.; Cui, Y. *Nat. Nanotechnol.* **2008**, *3*, 477.
- (33) Hannon, J. B.; Kodambaka, S.; Ross, F. M.; Tromp, R. M. *Nature* **2006**, *440*, 69.
- (34) Morales, A. M.; Lieber, C. M. *Science* **1998**, *279*, 208.
- (35) Kodambaka, S.; Tersoff, J.; Reuter, M. C.; Ross, F. M. *Science* **2007**, *316*, 729.
- (36) Wang, Y.; Schmidt, V.; Senz, S.; Gösele, U. *Nat. Nanotechnol.* **2006**, *1*, 186.
- (37) Persson, A. I.; Larsson, M. W.; Stenström, S.; Ohlsson, B. J.; Samuelson, L.; Wallenberg, L. R. *Nat. Mater.* **2004**, *3*, 677.
- (38) Henry, C. R. *Prog. Surf. Sci.* **2005**, *80*, 92.
- (39) Lewis, L. J.; Jensen, P.; Combe, N.; Barrat, J. L. *Phys. Rev. B* **2000**, *61*, 16084.
- (40) Choi, K.; Choi, J. W.; Kim, D. Y.; Hwang, N. M. *Acta Mater.* **2000**, *48*, 3125.
- (41) Cagin, T.; Kimura, Y.; Qi, Y.; Li, H.; Ikeda, H.; Johnson, W. J.; Goddard III, W. A. *Mater. Res. Soc. Symp. Proc.* **1999**, *554*, 43.
- (42) Baletto, F.; Ferrando, R. *Rev. Mod. Phys.* **2005**, *77*, 371.
- (43) Lee, S. H.; Han, S. S.; Kang, J. K.; Ryu, J. H.; Lee, H. M. *Surf. Sci.* **2008**, *602*, 1433.
- (44) Luedtke, W. D.; Landman, U. *Phys. Rev. Lett.* **1999**, *82*, 3835.
- (45) Silly, F.; Castell, M. R. *Phys. Rev. Lett.* **2006**, *96*, No. 086104.
- (46) Cai, J.; Ye, Y. Y. *Phys. Rev. B* **1996**, *54*, 8398.